ELSEVIER

Materials Science and Engineering B44 (1997) 181–187

MATERIALS SCIENCE & ENGINEERING B

Defect inspection of wafers by laser scattering

Katsumi Takami *

Shonan Institute of Technology, 1-1-25 Tsujido-Nishikaigan, Fujisawa 251, Japan

Abstract

This paper reviews defect inspection methods and instruments for evaluating semiconductor wafers by using elastic light scattering. The discussion focuses on the following instrument characteristics: minimum detectable size for the adhering particle, inspection throughput, detectability of microroughness and detectability of crystal defects at the subsurface and in the volume. By analyzing the detection mechanisms of laser surface scanners, scatterometers and infrared tomography systems, the unique capabilities of elastic light scattering for defect detection are revealed. © 1997 Elsevier Science S.A.

Keywords: Defect detection; Elastic light scattering; Semiconductor wafers

1. Introduction

The inspection of defects on the surface, at the subsurface and in the bulk crystal of wafers plays an important role in the yield-improvement effort of compound semiconductor and silicon device manufacturing. From the viewpoint of device manufacturing, the detection of adhering particles on the surface is always important. In addition, from the viewpoint of wafer production, the measurement of crystal defects in both the subsurface and the bulk regions, as well as of surface microroughness, is becoming increasingly important.

Until now, numerous inspection methods have been applied to detecting, locating and sizing the defects, e.g., electron beam, X-ray and optical methods. Among these, the elastic light scattering method has unique performance characteristics. While its sensitivity, accuracy and reliability are not sufficient from the standpoint of a detailed physical investigation, laser scattering is capable of detecting fine crystal defects as well as both fine particles and microroughness on wafers. Accordingly, it is assumed that the laser scattering method has intrinsic capabilities suitable for practical use in the semiconductor manufacturing processes.

This paper aims at reviewing commercially available instruments based on laser scattering methods by critically reviewing published literature.

* Corresponding author. Tel.: +81 0466 344111; fax: +81 0466 349527.

PII S0921-5107(96)01745-X

2. Practical classification of imperfections in wafers and optical detection methods for defects

Fig. 1 schematically illustrates the kinds of defects which influence production yield, and Table 1, comparing elastic light scattering with other optical methods, shows the capabilities appropriate for practical use.

Intending to be helpful to users of instruments, this paper will deal mainly with the basic instrument concept. Accordingly, physical considerations for data obtained with the instrument will be omitted, and appropriate literature cited.

3. Laser scattering by adhering particles on wafers

A typical configuration of an instrument utilizing laser scattering is shown in Fig. 2. When the incident laser beam illuminates an adhering particle on the surface, light scatter occurs as described below and the scattered light is detected by a photodetector after collection by the optical aperture over a solid angle of ω_c. Two-dimensional inspection of a wafer is made by a spiral scan of the wafer, or by an x-axis scan of the laser beam plus a y-axis scan of the wafer.

A freely suspended particle in a homogeneous medium simply scatters light in accordance with the Mie theory [4]. When the particle is irradiated by a laser beam, the intensity of the scattered light depends on the following parameters: (1) the size of the particle with respect to the laser wavelength, (2) the state of

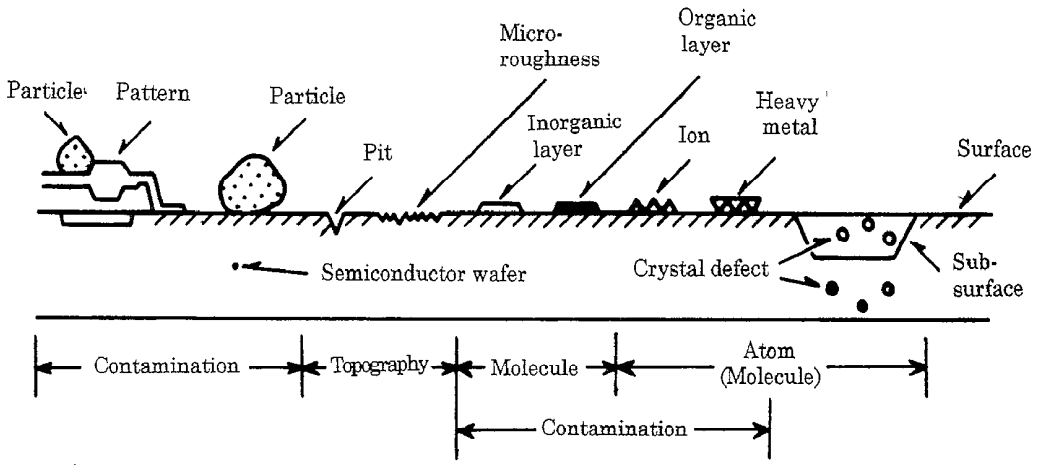

Fig. 1. Schematic classification of imperfections of a semiconductor wafer.

Table 1
Typical optical inspection methods for imperfections of semiconductors

Sample	Location	Imperfection	Methods
Mirror wafer	Surface	Particle, pit, scratch	Elastic light scarter (including visual inspection), optical microscope
		Microroughness	Elastic light scatter, phase shifting microscope [1], differential interference contrast microscope [1]
	Subsurface	Crystal defect	Elastic light scatter, PL, PAS, photovoltaic effect, thermal wave
	Volume	Crystal defect	IR light scatter, PL, PAS, Absorption, Photo-thermal radiation, Raman scatter
Patterned wafer	Pattern	Particle, pattern defect	Elastic light scatter, optical microscope, diffraction [2], depolarization [3]

PL, photoluminescence; PAS, photoacoustic spectroscopy.

polarization, (3) particle shape and (4) the particle index of refraction with respect to the surrounding medium.

However, in the case of an adhering particle on a wafer, features of the scattering become extremely complicated due to the complex boundary conditions of the surface, in addition to the parameters mentioned above.

Several authors [5–7] have proposed mathematical models on the basis of the Mie theory, together with experimental verification using standard particles, i.e., polystyrene latex spheres (PSL). Such theoretical studies elucidate the origin of detection errors when measuring real-world adhering particles [8] on compound semiconductor wafers. However, sufficient agreement between the models and the experimental data has not yet been obtained.

4. Improvement of detectability for adhering particles

4.1. Sensitivity (lower detection limit)

In order to detect as small a particle as possible, the scattered intensity caused by an adhering particle versus the noise component of the light intensity, i.e., an S/N ratio, should be taken into account. When a PMT (photomultiplier tube) is adopted as a photodetector (see Fig. 2), the S/N ratio is given approximately by Eq. (1).

$$\left(\frac{S}{N}\right)_{\text{power}} = \left(\frac{S}{N}\right)^2_{\text{amplitude}} = k_0 \frac{S_\lambda^2 I_S^2}{S_\lambda (I_S + I_B) + i_D} \frac{1}{\Delta B} \tag{1}$$

where $I_S = F(\pi d/\lambda, n, \theta_S, \psi_S)\omega_c I_i$, and where k_0 is a constant, S_λ is the spectral sensitivity of the PMT, I_S is the scattered light intensity by an adhering particle, I_B is the background light intensity, i_D is the dark current of the PMT, ΔB is the frequency band width of the electronics, d is the particle diameter, λ is the laser wavelength, n is the particle refractive index with respect to the surrounding medium, θ_S is the in-plane scatter angle (θ), ψ_S is the off-plane scatter angle (ψ), ω_c is the solid angle of the scattered light collecting optics and I_i is the incident beam intensity. The detailed functional dependencies of I_S can be derived from the Mie equation or Maxwell's equation [7].

One possible definition of the sensitivity of the instrument is the minimum detectable size (MDS), or noise equivalent size, which can be defined as the diameter of a deposited PSL sphere, yielding an S/N ratio of unity. Accordingly, in order to minimize the MDS, or to

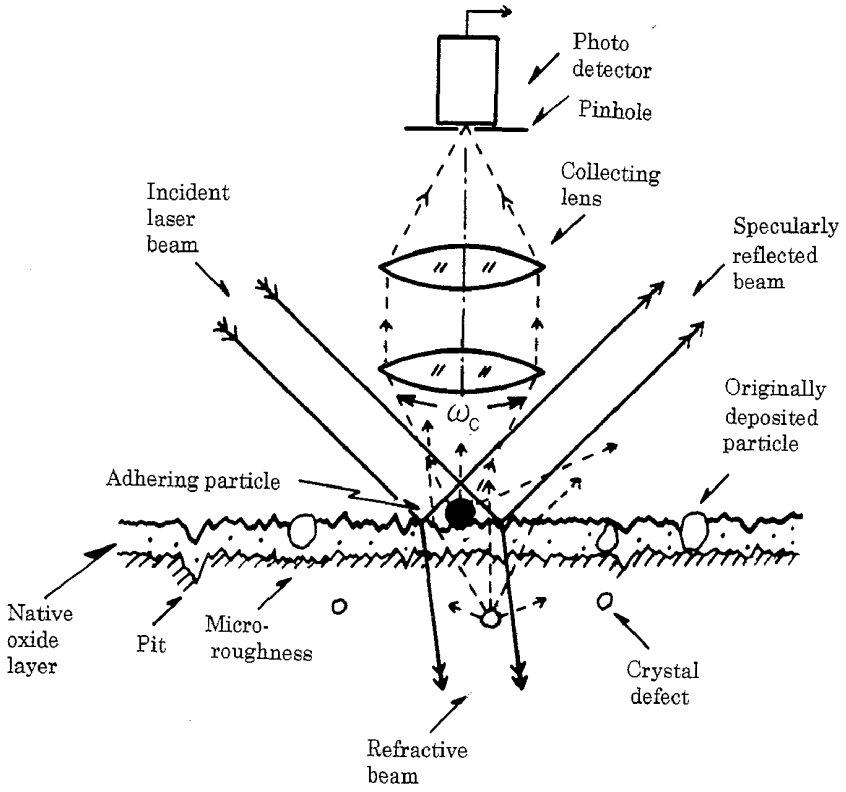

Fig. 2. Basic configuration of instrument for defect detection of wafers.

maximize the S/N ratio, an increase in I_S should be made, together with a decrease in I_B and ΔB. Here, it is assumed that i_D is negligible compared with $S_\lambda(I_S + I_B)$.

At present, all instrument manufacturers are concentrating on increasing the S/N ratio by enlarging ω_c, employing various optical features. Fig. 3 illustrates the configuration of scattered light collecting optics used in practice which maximizes ω_c.

Moreover, for the increase of the S/N ratio, I_B becomes significant in contrast to the situation of an airborne particle counter, i.e., a freely suspended particle. Referring to Fig. 2, I_B is the summation of all scattered light caused by microroughness, pits, originally deposited fine particles, and crystal defects at the subsurface. The most serious factor among these background components is the scattered light due to micro-roughness. This scatter thus ultimately determines the MDS [9], whereas for an airborne particle counter, Rayleigh scatter by the carrier gas (air molecules) dominates the lower detection limit [3].

For reference, the nominal MDS of the commercially available instruments is given in Table 2.

In addition, the particles deposited on an LSI pattern can be detected by polarized laser scattering, details of which may be found in the literature [3].

4.2. Inspection throughput

In the device manufacturing process, one needs to inspect the imperfections of a surface of large area (150–200 mm in diameter) within a limited time; namely, an increase in the inspection throughput (scan rate) is desired. However, the MDS and the inspection throughput yield incompatible optimization design criteria for the instrument [10]. For such incompatible parameters, it is convenient to introduce the evaluation factor, η_S, as follows [3]:

$$\eta_S = \frac{\text{Inspection speed}}{\text{Sectional area of MDS}} = \frac{(\pi D^2/4T)}{(\pi d_m^2/4)} = \frac{(D/d_m)^2}{T} \quad [1/s] \tag{2}$$

where D is the wafer diameter, T is the inspection time, and d_m is the MDS in diameter. As is evident from Table 2, η_S indicates a figure of merit, or intrinsic power of the instrument, the characteristics of which are predominantly determined by the optical configuration shown in Fig. 3.

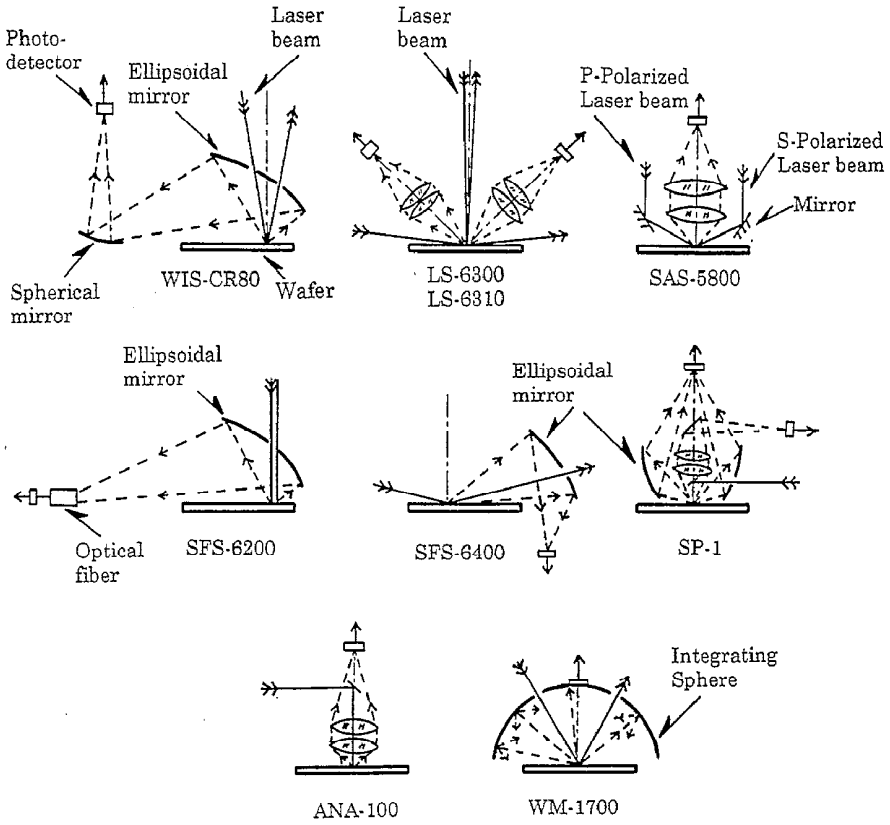

Fig. 3. Scattered light collecting optics developed by instrument manufacturers.

Table 2
Basic characteristics of surface inspection instruments[a]

Manufacturer	Model	Nominal MDS[b] (μm)	Inspection time (s per 6″ wafer)	η_S ($\times 10^9$)	Remarks
Estek	WIS-9000	0.10	60	1.1	—
	WIS-CR80	0.10	28	2.3	—
Hitachi DECO	LS-6300	0.09	35	2.3	—
	LS-6310	0.15	35	0.8	Oblique irradiation
PMS	SAS-5800	0.09	34	2.3	—
Tencor	SFS-6200	0.09	29	2.7	—
	SFS-6400	0.10	32	2.0	Oblique irradiation
Topcon	WM-1700	0.10	45	1.4	—

[a] Based on manufacturers' catalogs, or technical reports.
[b] MDS, minimum detectable particle size.

5. Detectability of microroughness

5.1. Definition of BRDF, microroughness and haze

Surface conditions, especially microroughness or haze of compound semiconductor and Si wafers, have become increasingly significant in terms of device performance [11]. Furthermore, microroughness indicates the efficacy of the adopted chemical–mechanical polishing of the wafer [1], or quality of the etching process [12]. Nevertheless, rigorous definition of microroughness and haze has not yet been established.

Referring to Fig. 4, BRDF (bi-directional reflectance distribution function) is defined as follows [13].

$$\mathrm{BRDF} \equiv \frac{\text{Differential radiance}}{\text{Differential irradiance}} \cong \frac{(\mathrm{d}P_S/\mathrm{d}\Omega_S)}{Pi\cos\theta i} \tag{3}$$

According to the American Society for Testing and Materials (ASTM), microroughness is defined as surface roughness components with a spacing between irregularities (spatial wavelengths) less than approximately 100 μm. Haze is defined as nonlocalized light scattering resulting from surface topography, or from dense concentrations of surface or near-surface imperfections. Accordingly, the instrument will indicate different values for microroughness and haze, although instrument manufacturers do not distinguish between these quantities. Again referring to Figs. 2 and 4, this value is given by

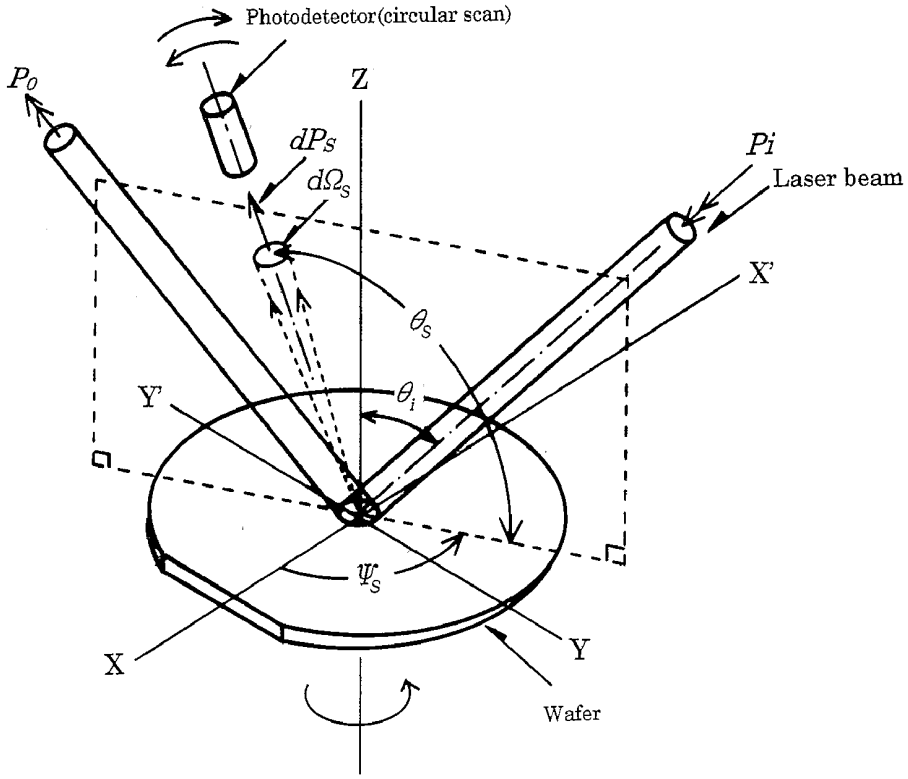

Fig. 4. Definition of BRDF and configuration of angle-resolved light scattering detection system.

$$\text{Microroughness} \equiv \frac{\text{Scattered power}}{\text{Incident power}} \cong \frac{\int_{\omega_c} (dP_S/d\Omega_S)\, d\omega}{Pi \cos \theta i} \cong \frac{(dP_S/d\Omega_S)\omega_c}{Pi \cos \theta i} \quad (4)$$

Therefore, the microroughness (or haze) value should be used only for relative measurements on a given instrument, due to the dependence on ω_c.

5.2. Scatterometer

A scatterometer, especially an ARLS (angle-resolved light scattering) system is a typical instrument for the measurement of BRDF. Fig. 4 depicts the basic configuration of an ARLS system in which the detecting angle θ_S and ψ_S for the scattered light are able to be finely adjusted [14]. This system is capable of providing unique information regarding the surface structure of crystals because of its high differential angular resolution and its sophisticated display (software) of PSD (power spectral density) [13].

5.3. Laser surface scanner

As previously mentioned (Figs. 2 and 3), scattered light caused by an adhering particle generates a pulse at the PMT of a laser scanning surface inspection system (LSS) and its pulse height corresponds to the particle size. Since microroughness can be thought of as the assembly of various sizes of ultra-fine particles (see Fig. 1), numerous pulses with low pulse heights appear at the PMT as illustrated in Fig. 5(A). Consequently, the PHA (pulse height analyzer) histogram shown in Fig. 5(B) depicts the distribution with respect to the grade of microroughness. Thus, the pulse-train component related only to microroughness is extracted by electronic filtering as the very low frequency wave, shown in Fig. 6. Accordingly, the DC level of this wave indicates the magnitude of microroughness.

By using such a DC level, Abe et al. [1] demonstrated the effectiveness of a topographical display of microroughness.

6. Detectability of crystal defects by laser scattering

6.1. Crystal defect topography by ultraviolet and visible light laser scattering

Light scattering is sensitive to differences or discontinuities in the refractive index (dielectric constant) in a crystal and to stress indices through piezo-optical effects [15]. Naturally, various crystal defects induce discontinuity in the refractive index. On the other hand, the penetration depth of the laser beam irradiated into the crystal depends on the laser wavelength. Therefore, by choosing the laser with the appropriate wavelength, crystal defects at the subsurface can be detected by the

scattering, in accordance with the penetration depth, under non-destructive and contact-free conditions.

Utilizing an LSS (model ANS-100, $\lambda = 325$ nm and 442 nm) shown in Fig. 3, Steigmeier and Auderset [16] discovered a close correlation of light scattering with the stacking fault density of a GaAs wafer, and established a three-dimensional topography display. Moreover, Abe et al. [17] also reported effective detection of OSF in Si wafers using a He–Ne laser (633 nm).

6.2. Crystal defect tomography by infrared laser scattering

Tomograhy of crystal defects in the bulk is effectively obtained by the infrared (IR) laser scattering method. An example of a commercially available instrument is shown in Fig. 7 [18].

In Fig. 7, horizontal irradiation of the laser beam and vertical scanning provides the tomograms of the vertical distribution of crystal defects.

Alternatively, when a polarized laser beam obliquely irradiates the surface under Brewster angle,

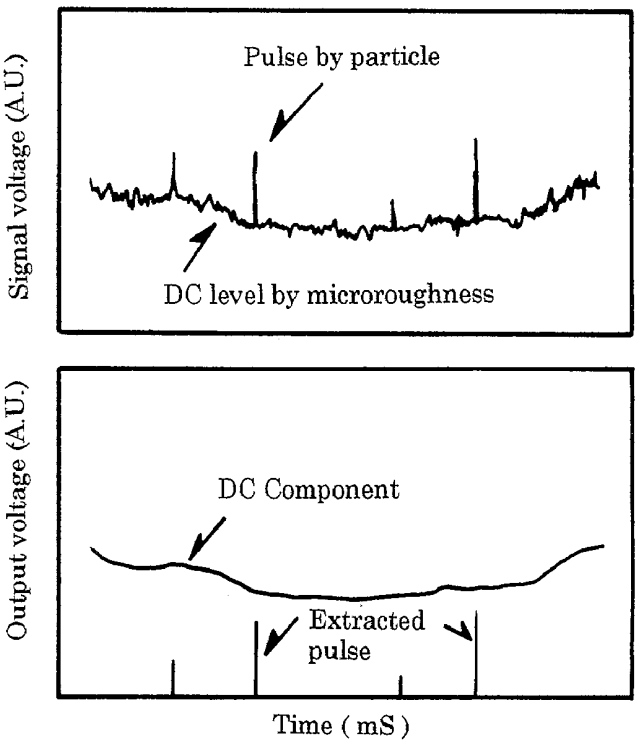

Fig. 6. Output wave forms of microroughness and filtered signal pulses.

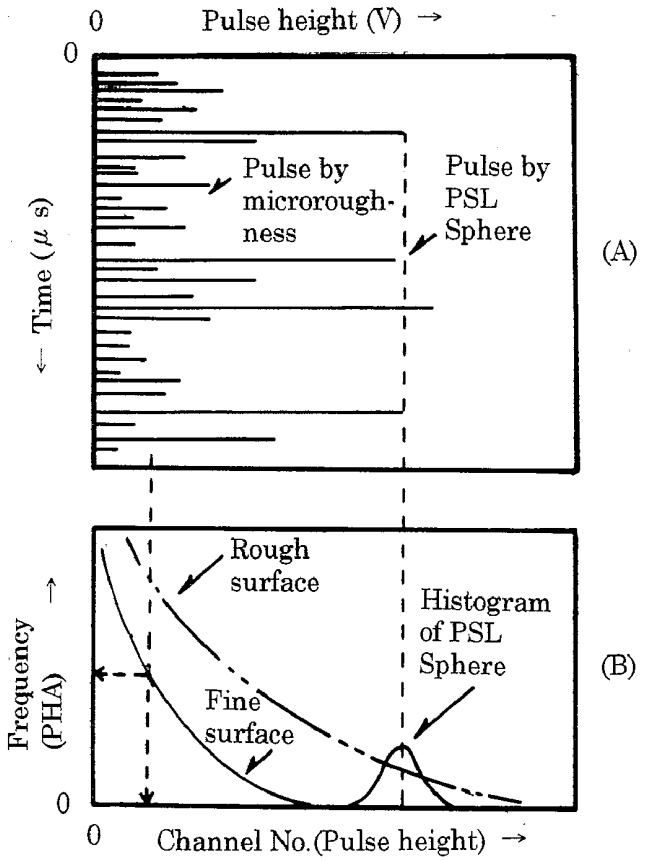

Fig. 5. Illustration of signal processing: (A) oscilloscope traces of pulses; (B) PHA histogram of pulses.

as also shown in Fig. 7, the p-component easily penetrates into the crystal, whereas almost all the s-component is reflected specularly from the surface. Therefore, by recording only the p-component of the scattered light, detection of defects in the volume can be made without any influence of surface conditions [18].

Oda et al. [19] discovered various properties of precipitates (e.g., As) in GaAs wafers by using IR tomography.

7. Conclusion

Instruments based on elastic light scattering, including the scatterometer, LSS topography systems and the IR laser tomography systems, have been presented, emphasizing issues of instrument engineering and application. The capabilities of the elastic light scattering methods are promising for practical application, especially if non-destructive and contact-free measurements are needed. Important reasonable aspects are sensitivity, high throughput for large area inspection, and adequate detectability of haze microroughness and crystal defects.

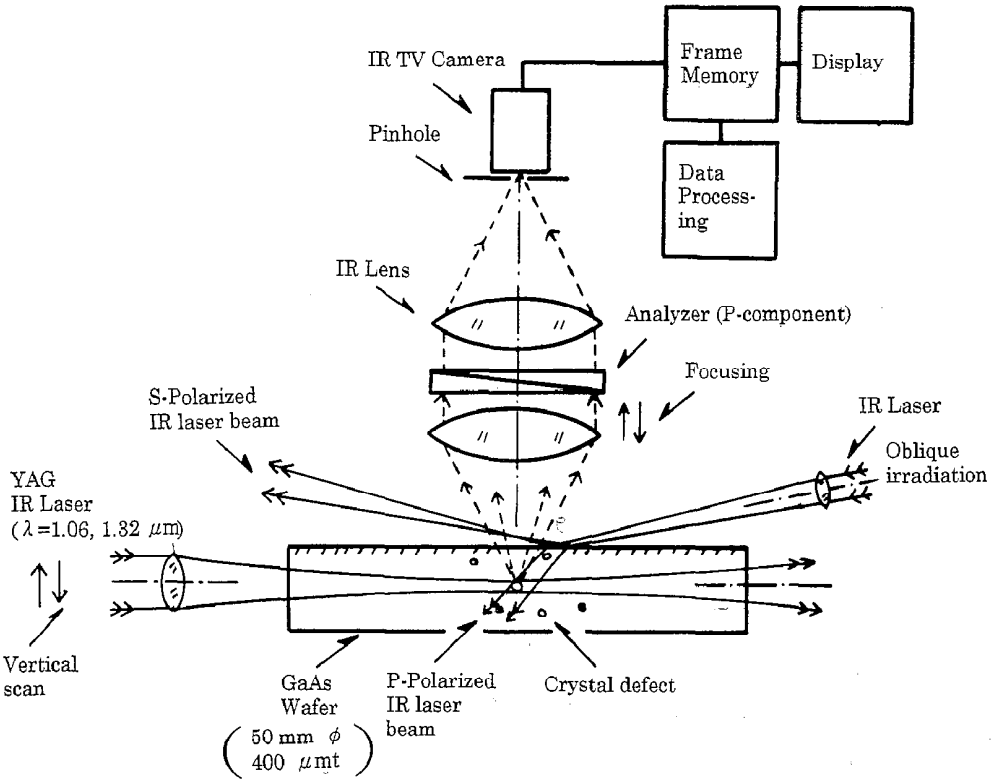

Fig. 7. Basic configuration of IR tomography system.

References

[1] T. Abe, E.F. Steigmeier, W. Hagleitner and A.J. Pidduck, *Jpn. J. Appl. Phys., 31* (1992) 721.

[2] N. Akiyama, F. Mizuno, M. Ikota and K. Takami, *Int. J. Jpn. Soc. Prec. Eng., 27* (1993) 361.

[3] K. Takami, T. Yachi, I. Hourai and Y. Yatsugake, *J. Aerosol Sci., 24* (1989) 457.

[4] H.C. van de Hulst, *Light Scattering by Small Particles*, Dover, New York, 1981.

[5] G.L. Wojcik, D.K. Vaugh and K.L. Galbraith, *SPIE, 744* (1987) 21.

[6] B.R. Locke and R.P. Donovan, *J. Electrochem. Soc., 134* (1987) 1763.

[7] H. Lee, S. Chae, Y. Ye, D.Y.H. Pui and G.L. Wojcik, *Aerosol Sci. Technol, 14* (1991) 177.

[8] S. Chae, H. Lee and Y.H. Liu, *Proc. Inst. Environ. Sci.*, (1992) 271.

[9] S. Piyooz, L.W. Shive, I.J. Malik and A.C. Martin, *Microcontamination, 11* (1993) 21.

[10] K. Takami, *Proc. 5th Meet. Lightwave Sensing Technology (Jpn. Soc. Appl. Phys.), Makuhari, Chiba, Japan, 24 May, 1990*, p. 103 (in Japanese).

[11] T. Ohmi, M. Miyashita, M. Itano, T. Imaoka and I. Kawanabe, *IEEE Trans. Electron Devices, 39* (1992) 537.

[12] E. Morita, J. Ryuta, T. Tanaka and Y. Shimanuki, *MRS Symp. Proc., 259* (1992) 161.

[13] J.C. Stover, *Optical Scattering—Measurement and Analysis*, McGraw-Hill, New York, 1990.

[14] K. Izunome, Y. Saito and H. Kubota, *Jpn. J. Appl. Phys., 31* (1992) L1277.

[15] T. Lu, K. Toyoda, N. Nango and T. Ogawa, *J. Cryst. Growth, 108* (1991) 482.

[16] E.F. Steigmeier and H. Auderset, *Appl. Phys. A, 50* (1990) 531.

[17] T. Abe, H. Takeno and S. Ushio, *Extended abstract, Surface Roughness and Scattering Topical Meet. (OSA), Tucson, AZ, USA, 1–3 June 1992*, 1992 Tech. Digest Ser., Vol. 14, p. 35.

[18] K. Moriya, A. Yazaki and K. Hirai, *Jpn. J. Appl. Phys., 34* (1995) 5721.

[19] O. Oda, H. Yamamoto, M. Seiwa, G. Kano, T. Inoue, M. Mori, H. Shimakura and M. Oyake, *Semicond. Sci. Technol., 7* (1992) A215.